Desalination and Water Treatment
www.deswater.com
doi: 10.1080/19443994.2014.895781

54 (2015) 1754–1769
May

Taylor & Francis
Taylor & Francis Group

Adsorption of anionic dye on natural and organophilic clays: effect of textile dyeing additives

Abidi Nejib[a,b], Duplay Joelle[b,*], Ayari Fadhila[a], Gangloff Sophie[b], Trabelsi-Ayadi Malika[a]

[a]*LACREsNE, Faculté des Sciences de Bizerte, Zarzouna 7021, Bizerte, Tunisia*
[b]*LHyGeS—UMR 7517 CNRS, EOST/UdS, 1 rue Blessig 67084 Strasbourg, France, Tel. +33 3 68 85 04 24;*
email: jduplay@unistra.fr

Received 21 November 2013; Accepted 22 January 2014

ABSTRACT

The adsorption of Reactive Red 120 (RR120) onto natural and organophilic clays was investigated in aqueous solution in a batch system with respect to contact time, initial dye concentration, initial pH, and additives from textile dyeing industrial effluents. The results showed that the organophilic clay fixed more RR120 dye molecules than the natural clay when additives are not present. The adsorption kinetics was found to follow the pseudo-second-order model. Dye molecules formed a monolayer over the homogenous surface of the modified and unmodified adsorbent. When textile dyeing chemicals were added, the amount of dye adsorbed onto clay varied depending on the nature of the added chemical. However, on the overall, adsorption on the natural unmodified clay was enhanced, whereas it remained reduced or at least unchanged in case of the organophilic clay. Adsorption on both clays was enhanced when all additives were present together. Adsorption was also enhanced when non-clay minerals (>2 μm fraction) were present in the unmodified bulk clay sample. Fourier transform infrared spectroscopy analyses showed strong evidence of interactions between RR120 dye and clay and also with additives.

Keywords: Adsorption; Anionic dye; Textile dyeing additives; Organo-clay; Surfactant

1. Introduction

Dyes are used in many industries, such as textile, paper, leather, food, and cosmetic industries [1], and are known to be toxic to organisms when released in the aquatic ecosystem. They may alter the antioxidant defense [2], act as endocrine disrupting agents [3], induce cell death, chromosomal aberrations, nuclear alteration, and micronuclei [4,5]. In their review, Combes and Haveland-Smith [6] report that synthetic dyes from the three major structural classes exhibit genotoxicity. Moreover, dyes are persistent in the environment. The Azo dyes for example, cannot be degraded by conventional aerobic sewage treatment plants because they are resistant to biological oxidative degradation [7]. The azo bonds can be reduced, however, producing aromatic amines which are resistant to further degradation and may thus be still toxic or genotoxic [8]. Drumond Chequer et al. [9] for example, studied azo dye Disperse Red 1 which has already been assigned as mutagenic in different cell systems; they evidenced in addition, that the dye still had

---

[*] Corresponding author.

mutagenic activity for the Salmonella/microsome assay after an oxidation or a reduction process. Another disturbing effect is related to the color persistence. The colored liquid waste released in waters impedes the sun light transmittance, thereby reducing photosynthesis and disturbing the natural balance of water life and the food chain [10–12]. The classic treatment method for removal of dyes in wastewater includes two steps: the first is a physico-chemical treatment which is characterized by the addition of chemical reagents (aluminum chloride and ferric chloride) and the second is biological which is carried out using activated sludge under aeration [13]. The difficulty with the use of coagulation–flocculation agent lies in the fact that it is virtually impossible to eliminate the total amount of dye in the water, in addition to poor settleability of formed flakes [14]. The biological treatment processes are rarely solely used because of the low biodegradability of dyes. Other physico-chemical treatments are used: they include chlorination, ozonation, reverse osmosis, ion-exchange, electrochemical [15], photochemical, and photocatalytic degradations [16]. However, all these methods are significantly different in terms of color removal, operation, and financial cost [17,18].

Among liquid waste treatment methods, adsorption is a technique relatively used and easy to implement. Activated carbon is the most widely used adsorbent because of its high adsorption capacity for organic materials [19]. This adsorbent however has a high cost and is difficult to regenerate. Therefore, search of more efficient and less costly adsorbents has attracted much interest. In the last few years, tests were performed on various kinds of adsorbents, such as rice husk [20–22], sugarcane bagasse [23], fibrous biomass [24], neem leaf [25,26], apple pomace, and wheat straw [27], reverse micelles [28], and various other adsorbents [29–48] for the removal of organic pollutants from wastewater. In this context, clays have gained a lot of interest because of their efficiency in the adsorption of organic and inorganic ions and molecules, their affordable cost and abundance [49]. Several studies showed that clay minerals, when modified by organic surfactants, become suitable materials for anions retention [50–54]. Therefore, the surface modification of clay minerals by intercalation of cationic surfactants, as for example quaternary ammonium compounds, has received great interest. It changes the surface properties from hydrophilic to hydrophobic and increases interlayer spaces, and thus the anions adsorption capacity.

Previous studies pointed out the efficient adsorption of anionic dye Reactive Red 120 (RR120) by raw untreated Fouchana clay composed of smectite, kaolinite, and illite [55–58]. That natural untreated Fouchana clay also proved its efficiency in color removal from effluents containing various additives mixed with anionic dyes [55]. This suggests that additives do not hinder the adsorption of anionic dye on raw clay and even contribute to a more efficient color removal. In the latter case, textile dyeing additives would act as surfactants and modify the raw clay surface and consequently enhance dye adsorption on these modified surfaces.

In order to test this hypothesis we investigated the effect of additives from a textile dyeing industry on color removal by raw Fouchana clay and compared its adsorption capacity with that of Fouchana clay modified by a cationic surfactant (hexadecyltrimethylammonium bromide: HDTMA-bromide). Various techniques were used in the characterization of synthesized HDTMA-clay and natural clay, including X-ray diffraction (XRD) and Fourier transform infrared spectroscopy (FTIR). Batch experiments were performed for RR120 dye adsorption on natural and modified Fouchana clay testing the influence of contact time, initial pH, initial dye concentration, and additives from textile dyeing industry.

2. Materials and methods

2.1. Adsorbent

2.1.1. Natural clay

Fouchana clay deposit is situated in the region of Fouchana, northeast of Tunisia. The clay mineralogical composition was determined on the <2 μm fraction by XRD analysis. The proportions of each clay type were estimated by the Reference Intensity Ratio method using the HighScore software (Table 1). Fouchana clay

Table 1
Physical and chemical characteristics of the Fouchana clay

Parameter	Unit	Fouchana clay <2 m
Specific surface	$m^2\,g^{-1}$	80
CECp	$C\,mol\,kg^{-1}$	34.3
PZNPC	–	3.4
Smectite	%	60
Kaolinite	%	30
Illite	%	10
SiO_2	% (wt.)	52.1
CaO	% (wt.)	1.01
Na_2O	% (wt.)	0.02
Al_2O_3	% (wt.)	22.7
MgO	% (wt.)	2.17
Fe_2O_3	% (wt.)	9.15
K_2O	% (wt.)	2.46
TiO_2	% (wt.)	0.92

is a mixture of expanding clay (50% smectite and 10% interstratified illite/smectite) and non-expanding clay (30% kaolinite and 10% illite). The non-clay minerals are mainly quartz (40%), calcite (10%), and gypsum (10%). The specific surface area (Ss) and cation-exchange capacity (CEC) were measured by the BET [59] and Metson methods, respectively (AFNOR NF X 31–130) [60]. The global Ss area is rather high owing to the proportion of expanding clay, and the CEC has an average value reflecting the mixture of clay species (Table 1). The chemical composition obtained after borate fusion by ICP-AES (Jobin Yvon JY 124) shows high silicium and aluminum contents due to the dominant quartz and aluminum-rich phyllosilicates composing Fouchana clay (Table 1).

2.1.2. Modified clay

The <2 μm size fraction of Fouchana clay was purified by repeated cation exchange in NaCl solution (1 M) followed by washing, sedimentation, and dialyzing operations [61]. The organo-clay was then prepared by slow addition of HDTMA-bromide solution into a suspension in water of purified clay. The procedure adopted is described by Baskaralingam [62] and consisted of 24 h—stirring at room temperature followed by washing with distilled water until a negative bromide test with 0.1 M $AgNO_3$ was obtained. The sample was finally dried at 60°C.

2.2. Adsorbate

The anionic dye RR120 chosen in this work was provided by a Tunisian cotton dyeing industry. The characteristics and chemical structure of RR120 dye are listed in Table 2.

2.3. Textile dyeing additives

The textile dyeing set of additives chosen for this study is a selection of chemicals used in the same Tunisian industry as for RR120 dye. They are of different chemical nature and ionic form (Table 3). CHT Catalase is an enzymatic auxiliary used to destroy residual peroxide after textile bleaching. Kollasol is a hydrophilic silicone surface-active substance mixed with higher alcohols: it acts as a de-aerator and penetration accelerator. It is used to cationize cellulose before dyeing with anionic dyes [63,64]. Meropan DPE is a polycarboxylic acid with modified phosphonates; it has the role of protective colloid with sequestering properties for hardening agents when prewashing and dyeing cellulose and cellulose fiber mixtures. Cotoblanc sel 200 is a mixture of sequestering agent and polymers with affinity to dyes; it removes unfixed reactive dye from cellulose substrates. Bactosol CA LIQ C is a bacterial enzyme for cellulose in acidic conditions; it improves surface appearance and aids in achieving a stonewashed effect with less stones. Duralkan FSR is a nitrogenated polycondensate, formaldehyde and metal free. It is a fixing agent to improve wet fastness of direct and reactive dyeing.

2.4. Methods

2.4.1. Characterization of the adsorbent

XRD analyses were performed on a Brüker D5000 diffractometer with Cu anticathode at 40 kV voltage

Table 2
Physical properties and molecular structure of RR120

Dye name	Reactive Red 120
Chemical formula	$C_{44}H_{24}C_{12}N_{14}Na_6O_{20}S_6$
Molecular weight (g/mol)	1338.04
λ max	535 nm
Molecular structure	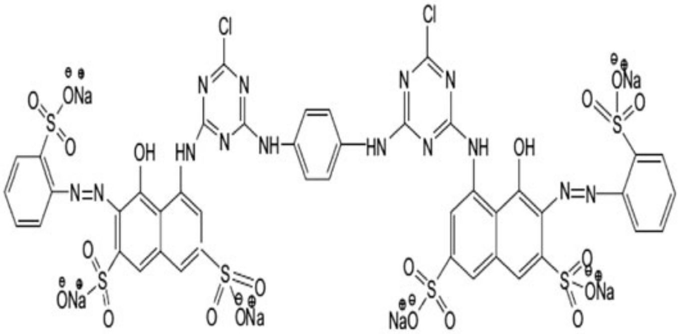
Water solubility	70 (g /L)
Class	Diazo (–N=N– bond)

and 30 mA current. XRD patterns of oriented samples were collected from 3° to 65° scanning angle, 0.02 s upward step, and a wave length $\lambda K\alpha1 = 1.54056$ Å.

The infrared analysis of the <2 μm clay before and after dye adsorption was carried out on a Perkin–Elmer FT-IR spectrophotometer. The spectra were recorded in the region from 400 to 4,000 cm^{-1} with a spectral resolution of 2 cm^{-1}. KBr pellets were prepared by mixing 10 wt.% clay with 90 wt.% KBr and by pressing.

The pH-dependent surface charge of the clays was determined by potentiometric titration under CO_2− free atmosphere using NaCl as electrolyte to maintain a constant ionic strength of 0.01 or 0.1 M. Prior to the titration, the suspensions containing 4 g clay were vigorously stirred and bubbled with CO_2− and O_2− free argon (Sigma Oxiclear cartridge) (905 Titrando Metrohm) for half an hour. The potentiometric titration was performed by means of an automatic titrator system Basic Titrino 794 (Metrohm 2.794.0010) with combined glass electrode (Metrohm 6.0234.500, Long Life) filled with 0.1 M NaCl in water.

The data were acquired with the help of the Tiamo light 1.2 (Metrohm AG Ltd, Herisau, Switzerland) soft-

Table 3
Physical and chemical characteristics of textile dyeing additives used in this study

Additives	Chemical name	Chemical formula	Molecular structure	Molecular weight ($g\ mol^{-1}$)
CHT Catalase	9-Ethyl-6,11-dihydro-6,6-dimethyl-8-[4-(4-morpholinyl)-1-piperidinyl]-11-oxo-5H-benzo[b]carbazole-3-carbonitrile CAS Number 86352-20-7	$C_{30}H_{34}N_4O_2$	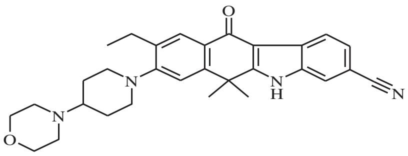	482.62
Kollasol	3-Chloro-2-hydroxypropyltrimethyl ammonium chloride CAS Number 56780-58-6	$C_6H_{15}Cl_2NO$	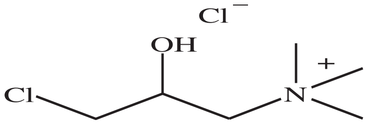	188.12
Meropan DPE	DPE-ethyl bromide CAS Number 9015-54-7	$C_{23}H_{32}BrNO_3$	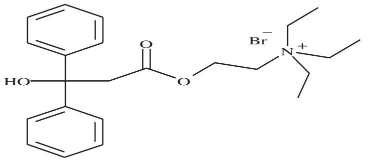	449.904
Bactosol CA LIQ C	2-Bromo-2-nitropropane-1,3-diol CAS Number 37259-58-8	$C_3H_6BrNO_4$	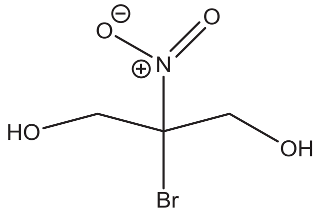	199.988
Cotoblanc Sel 200	TRY 200 CAS Number 136626-78-3	$C_{20}H_{32}O_5$	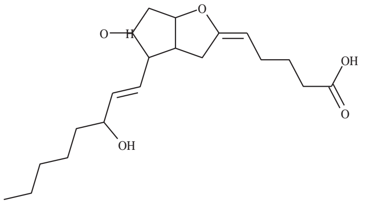	352
Duralkan FSR	3H-Indole-5-carboxylicacid, 2-[2-[4-[(4-ethoxyphenyl)methyl amino]phenyl] ethenyl]-3,3-dimethyl-,methyl ester CAS Number 86352-20-7	$C_{29}H_{30}N_2O_3$	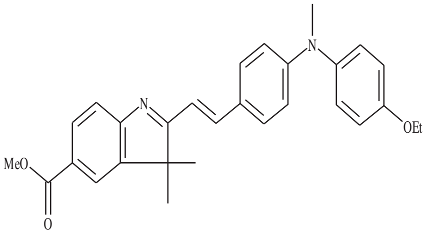	454

Table 4
Adsorption kinetic parameters of RR120 dye onto natural-Fouchana and HDTMA-Fouchana (pH = 6, T = 25 °C)

	Pseudo-first-order			Pseudo-second-order				Elovich			Intra-particle diffusion		
	q_e (mg/g)	K_1 (1/min)	R^2	q_e (g/mg min)	K_2 (mg/g min)	h (mg/g min)	R^2	α (mg/g min)	β (g/mg)	R^2	C (mg/g)	K_{ip} (mg/g min$^{1/2}$)	R^2
Natural-Fouchana	4.53	0.033	0.918	7.23	0.006	0.313	0.985	0.28	1.75	0.927	1.66	0.43	0.85
HDTMA-Fouchana	8.16	0.054	0.729	22.88	0.0081	4.248	0.998	0.049	3.87	0.877	13.48	0.931	0.757

ware, with the following characteristics: MET U (monotonous equivalence titration) method, increment 2 μL, dosing increments rate 2 mL/min, maximum drift signal 1.5 mV/min. To obtain a titration curve in the pH range between 3 and 9, the total proton/hydroxide consumption by the samples was calculated by the difference between the added amounts of titrants and the final concentration of protons calculated from the equilibrium pH. On the raw titration curves pH is represented vs. the concentration of added titrant (Ca and Cb for acid and base, respectively), the acid being set positive and the base negative (Ca − Cb). Some trials were duplicated to examine the analytical reproducibility.

2.4.2. Batch experiments

The adsorption of RR120 on natural (Fouchana) and modified (HDTMA-Fouchana) clays was investigated in aqueous solution in a batch system with respect to contact time, initial dye concentration, initial pH, and textile dyeing additives. The experiments were performed at room temperature (25 °C) with a constant solution volume (V) of 100 mL. Preliminary experiments at a dye concentration of 30 mg/L were carried out to determine the mass of natural clay at which a maximum of dye molecules was removed from solution. Therefore, all experiments were conducted with a mass of adsorbent set at 3 g. The flasks were agitated on a mechanical shaker for 1 h to ensure that the equilibrium was reached. The reaction mixture was centrifuged and the supernatant was analyzed by measuring the absorbance at the wavelength corresponding to the maximum absorbance. The amount of dye adsorbed by the sorbent at time $t - q_t$ (mg/g), was calculated using the following mass balance relationship
(Eq. (1)):

$$q_t = (C_0 - C_e) \times (V/m) \tag{1}$$

where C_0 is the initial concentration of the dye solutions (mg/L), and C_e is the equilibrium concentration of the dye solutions; q_t is the dye concentration on adsorbent at any time t (mg/g), V the volume of dye solution (mL), and m (g) the mass of sorbent.

2.4.3. Adsorption kinetics

The kinetics of RR120 adsorption onto natural (Fouchana) and modified (HDTMA-Fouchana) clays was investigated using four models: the pseudo-first-

Table 5
Langmuir and Freundlich isotherm constants for the adsorption of RR120 dye onto natural- and HDTMA-Fouchana clays without additives (pH = 6, $T = 25^\circ$C)

Models	Equation	Parameters Natural-Fouchana+RR120	Parameters Fouchana-HDTMA+RR120
Langmuir	$1/q_e = 1/(q_m K_L) \times (1/C_e) + 1/q_m$	q_m(mg/g) = 54.644 K_L (mg/L) = 0.0049 $R^2 = 0.9988$ SSQR = 0.12	q_m(mg/g) = 163.93 K_L (mg/L) = 0.0019 $R^2 = 0.997$ SSQR = 0.46
Freundlich	$q_e = K_F\, {C_e}^{1/n}$	$n = 1.039$ K_F(mg/g) = 0.604 $R^2 = 0.9565$ SSQR = 0.09	$n = 0.\ 86$ K_F(mg/g) = 1.46 $R^2 = 0.974$ SSQR = 0.6

Table 6
Initial solution pH conditions in adsorption experiments of this study

	Without additives		Clay and dye solution with additives						
	Dye solution	Clay and dye solution	Duralkan	Meropan	Cotoblanc	Bactosol	CHT Catalase	Kollasol	All additives
pH of initial solution	6	5.3	6.1	8.5	5.8	5.7	6.1	6.7	8.5

order, pseudo-second-order, Elovich, and intra-particle diffusion models.

The Lagergren pseudo-first-order equation is the following [65] (Eq. (2)):

$$\ln\,(q_e - q_e) = \ln\, q_e - K_1 t \tag{2}$$

where K_1 is the equilibrium rate constant of pseudo-first-order adsorption (1/min), q_e and q_t are the amounts of dyes adsorbed at equilibrium and at time t (mg/g).

The pseudo-second-order equation describes the process over the whole period of adsorption. The linear form is [66] (Eq. (3)):

$$\frac{t}{q_t} = \frac{1}{K_2 q_e^2} + \frac{t}{q_e} \tag{3}$$

where K_2 is the rate constant of adsorption, q_e is the amount of dye adsorbed at equilibrium (mol/g), and q_t is the amount of dye adsorbed at time t (mol/g).

The equilibrium adsorption capacity (q_e) and the second-order rate constant K_2 (g/mol min) can be determined experimentally from the slope and intercept of plot of t/qt vs. t if the initial adsorption rate is [67] (Eq. (4)):

$$h = K_2 q_e^2 \tag{4}$$

The intra-particle diffusion can be described by three consecutive steps: (i) the transport of adsorbate from the bulk solution to the outer surface of the adsorbent by molecular diffusion, (ii) the internal diffusion, the transport of adsorbate from the particles surface into interior sites, and (iii) the adsorption of the solute particles from the active sites into the interior surface of the pores.

The effect of intra-particle diffusion resistance on adsorption can be determined by the following relationship [68] (Eq. (5)):

$$q_t = K_{ip} t^{1/2} + C \tag{5}$$

where K_{ip} represents intra-particle diffusion rate constant (mg/g min$^{1/2}$) and C is a constant (mg/g) which gives information about the thickness of boundary layer. The plot of q_t vs. $t^{1/2}$ yields a straight line passing through the origin in case of intra-particle diffusion.

The linear form of Elovich equation is (Eq. (6)):

$$q_t = \frac{1}{\beta\, \ln(\alpha\beta)} + \frac{1}{\beta}\, \ln t \tag{6}$$

where α (mg/g min) is the initial adsorption rate constant and the parameter β (g/mg) is related to the extent of the surface coverage and activation energy for chemisorption [65,69]. The values of α and β can be calculated from the plot of q_t against $1/\ln t$.

2.4.4. Adsorption isotherms

In this study, two popular equilibrium isotherm models were tested to describe the experimental data, namely Langmuir [70,71] and Freundlich isotherm models [72]. The Langmuir isotherm model is based on the assumption that the maximum sorption capacity corresponds to full monolayer coverage of the solute molecules on the adsorbent surface, with no interaction between sorbed molecules. The linear form of Langmuir model is (Eq. (7)):

$$C_e/q_e = 1/q_m K_L + C_e/q_m \tag{7}$$

where C_e is the equilibrium concentration (mg/L), q_e the amount adsorbed at equilibrium (mg/g), q_m the adsorption capacity (mg/g) and K_L is a constant related to the affinity of the binding sites (L/mg). The values of q_m and K_L were calculated from the slope and intercept of the linear plots C_e/q_e vs. C_e which gives a straight line of slope $1/q_m$ which corresponds to complete monolayer coverage (mg/g) and the intercept is $1/q_m\ K_L$.

The Freundlich isotherm model [73] is an empirical equation and used to describe heterogeneous surfaces. The linear form of Freundlich model is (Eq. (8)):

$$\mathrm{Ln}(q_e) = \mathrm{Ln}(K_F) + 1/n\ \mathrm{Ln}(C_e) \tag{8}$$

where K_F and n are Freundlich constants and were calculated from the slope and intercept of the Freundlich plots ($\mathrm{Ln}(q_e)$ vs. $\mathrm{Ln}(C_e)$).

3. Results and discussion

3.1. Characterization of organo-clay

XRD patterns obtained for the natural untreated clay (Fouchana), the Na-exchanged purified sample (Na-Fouchana), and the modified clay (HDTMA-Fouchana) are given in Fig. 1. The position of the (0 0 1) reflection is recorded at 14.41 Å for Fouchana. That layer equidistance suggests that the smectite minerals are in the Ca-exchange form [74]. Na-Fouchana pattern shows a position of the (0 0 1) reflection (d = 12.64 Å) characteristic of a sodium-exchanged smectite. The HDTMA-Fouchana pattern compared to the others shows an increased d-spacing of 21.57 Å which indicates the intercalation of HDTMA molecules (Fig. 1). The d-spacing value is in agreement with those obtained by Slade and Gates [75] for various smectites.

The IR spectroscopic analysis performed on HDTMA-Fouchana produced vibration bands at 2,932 and 2,859 cm^{-1} corresponding to the C–H and C–H$_3$ vibrations, respectively, and a vibration band at 1,471 cm^{-1} corresponding to the N–R$_4$ vibration (Fig. 2). All these vibrations suggest the interaction of HDTMA with Fouchana clay.

3.2. Adsorption

3.2.1. Effect of contact time and kinetic study

The batch adsorption experiments were conducted at pH 6.0, at different contact times (20–120 min), for an initial concentration of RR120 dye of 80 mg/L. The adsorption capacity of RR120 increased with contact time rapidly for the first 10 min and thereafter it proceeded at a slower rate and finally reached equilibrium after 60 min for both clays (Fig. 3). The rapid adsorption during the first 10 min for Fouchana and HDTMA-Fouchana was probably due to the abundant availability of active sites on the clay surface, but with the gradual occupancy of these sites, the adsorption

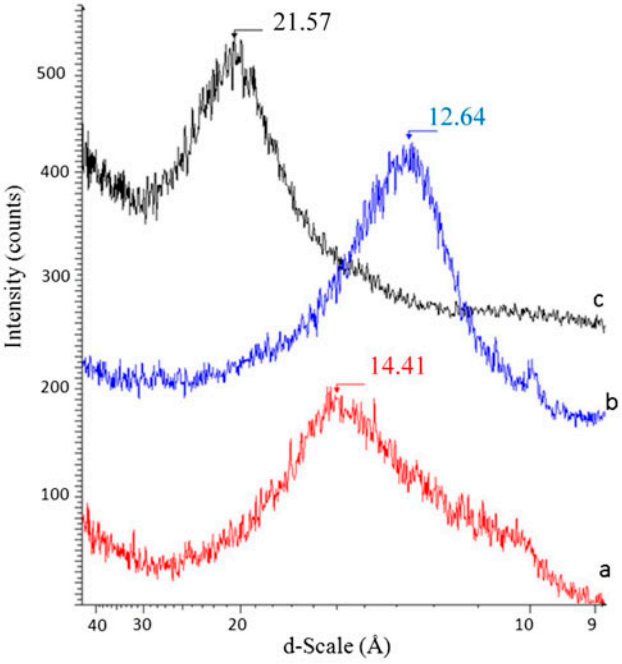

Fig. 1. XRD patterns of natural-Fouchana (a), Na-Fouchana (b), and HDTMA-Fouchana clays (c).

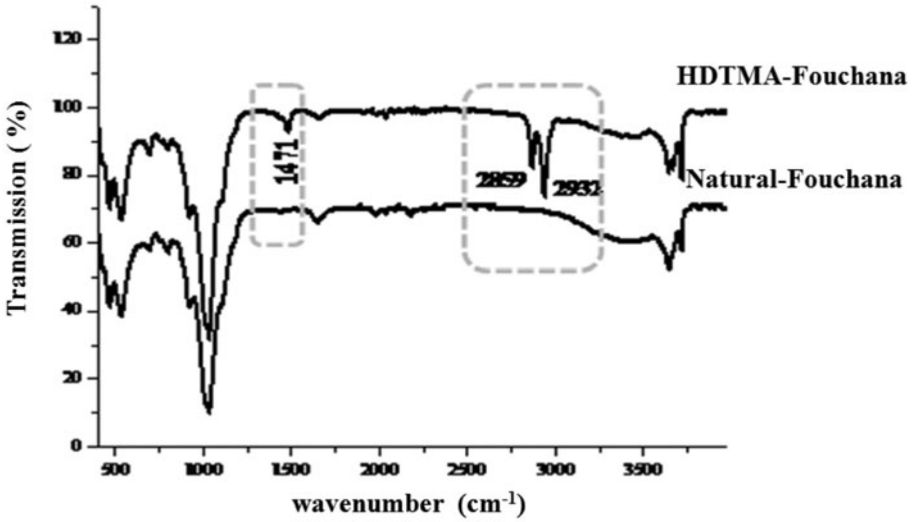

Fig. 2. IR spectra of natural-Fouchana and HDTMA-Fouchana clays.

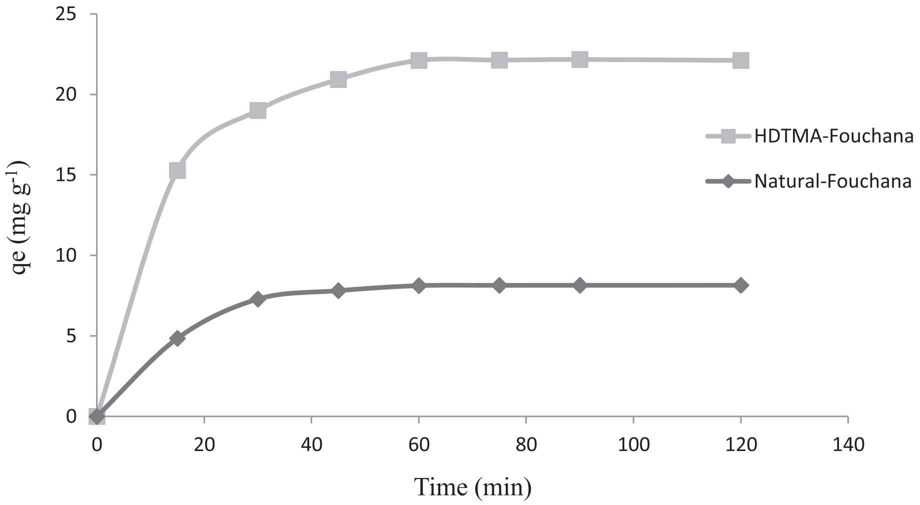

Fig. 3. Effect of contact time on adsorption of RR120 onto natural-Fouchana and HDTMA-Fouchana clays ($C_0 = 80\,\text{mg/L}$, pH = 6, $T = 25$°C).

became less efficient. The amount of dye adsorbed onto HDTMA-Fouchana was three times higher than for Fouchana which shows that HDTMA efficiently modified the clay surface charge and enhanced cationic adsorption site availability for RR120 anionic dye.

To investigate the solute uptake rate which controls the residence time of adsorbate uptake at the solid-solution interface, RR120 adsorption data were examined by the pseudo-first-order, pseudo-second-order, Elovich, and intra-particle kinetic models (Table 4). The results show that data are best fitted by the pseudo-second-order model as evidenced by high correlation coefficients (0.985 and 0.998 for the adsorptions onto Fouchana and Fouchana-HDTMA, respectively). Moreover, the amounts of adsorbed dye calculated by the pseudo-second-order model are very close to those recorded experimentally which further suggests that RR120 adsorption rate follows this model in both cases. The initial adsorption (h) is low in the case of Fouchana natural clay contrary to Fouchana-HDTMA for which adsorption process is rapid from the beginning. This is in relation with the higher availability of cationic adsorption sites in organo-clay, and thus a higher probability for adsorbent sites and dye molecules to be in contact.

3.2.2. Effect of pH

The effect of solution pH on RR120 dye adsorption onto Fouchana and HDTMA-Fouchana was investigated at pH conditions from 3 to 12. It should be noted that RR120 dye is not altered in that pH range as evidenced by potentiometric titration [58]. Moreover, the points of zero net proton charge of natural-Fouchana and Fouchana-HDTMA are, respectively, 3.4 and 4.1 which indicate that particle edges are dominantly negatively charged for higher pH values. As shown in Fig. 4, the adsorption of the anionic dye is dependent on pH. Although the adsorption capacity of organo-clay is still significantly higher than that of natural-Fouchana, whatever the pH value, the amount of removed dye decreases for both clays when pH increases, the maximum of adsorption being obtained in an acid medium (pH ≈ 3). This decrease going from an acidic to a basic medium is explained by the increase in negative charges of clay particles acting as repulsive forces towards the dye molecule SO_3 groups, and by the increase of OH^- ions which compete with RR120 dye anions in solution and disadvantage the setting of RR120 anions onto clay. The adsorption of RR120 dye onto organo-clay which is dominated by interlayer adsorption processes, however, does not drastically change when adsorption capacity on the edges decreases. In the case of Fouchana natural clay for which anion adsorption capacity is low and the adsorption process is probably mostly related to edges, the pH increase lowers significantly the amount of adsorbed dye.

These results are in agreement with other studies showing that pH plays an important role in the improvement of dye adsorption. This phenomenon was clearly observed for example in the adsorption of Rose sulfacid dye onto bentonite [76], Reactive Blue 19 dye [77], or AR1 acid dye [78] onto modified bentonites.

3.2.3. Effect of initial RR120 dye concentration

Batch experiments were carried out at different initial concentrations of RR120 dye from 10 to 120 mg/L and in the natural pH conditions of the initial solution (pH 6).

According to the classification of Sposito [79] adsorption isotherms are of L-type which are characterized by a slope increasing with the concentration of the substance in solution (Fig. 5). This is the result of a relatively high affinity for the solid phase to the adsorbed substance, coupled with a decrease in the number of adsorption sites. The amount of dye removed by HDTMA-Fouchana is about 22.8 mg/g, much higher than that removed by the unmodified clay (about 5.65 mg/g). It appears that the maximum initial dye concentration beyond which the unmodified clay is unable to adsorb more dye is limited at 30 mg/L. Concerning HDTMA-Fouchana it is limited at 80 mg/L. Indeed, interaction of alkylammonium with the clay network reduces the surface energy of the clay layer charge to make it compatible with the matrix of RR120 dye, thus improving the attraction between the dye and clay. In addition, the alkylammonium ions are carriers of functional groups which can react with the matrix of the dye.

Several studies in the literature, report on the highly efficient adsorption of anionic dye by organo-clays compared to the crude clay. Among them, Ikhtiyarova et al. [77] observed that HDTMA-modified bentonite adsorbs three times more anionic dye than natural bentonite. Juang et al. [78] compared the acid

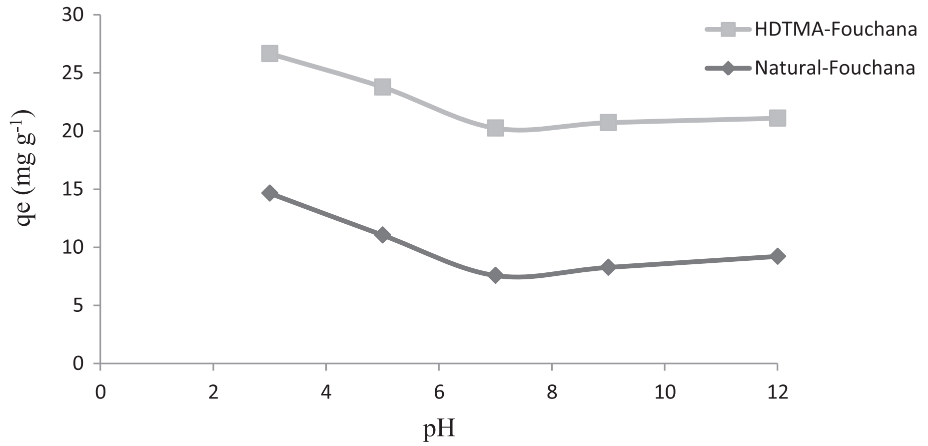

Fig. 4. Effect of pH on adsorption of RR120 onto natural-Fouchana and HDTMA-Fouchana ($C_0 = 80$ mg/L, $T = 25$°C).

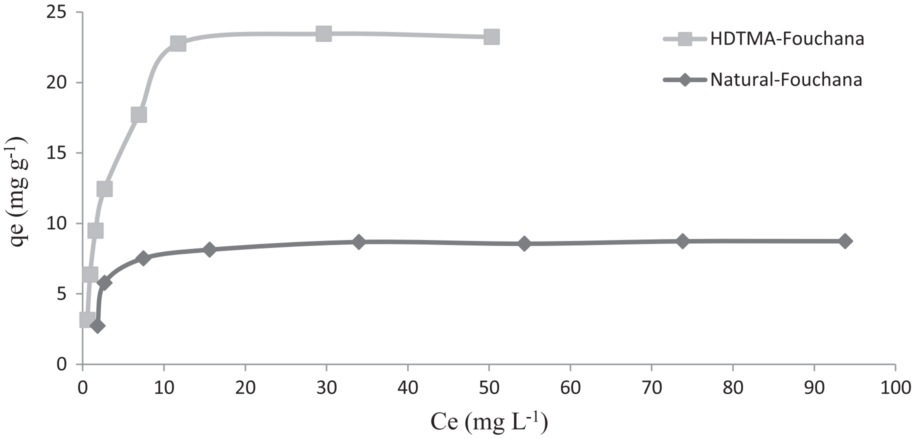

Fig. 5. Effect of initial RR120 dye concentration on the adsorption onto Fouchana and HDTMA-Fouchana clays (pH = 6, *T* = 25˚C).

red dye (Amido Naphthol Red G) adsorption capacity of Ca-montmorillonite and its modified form. The amount adsorbed for the latter was 10 times that of the natural clay. Anionic dye adsorption enhancement in the same order of magnitude was also reported for organo-montmorillonite with RR141 dye [80] or Serbian organo-modified bentonites with RB5 dye [81]. Organo-vermiculite also exhibits high adsorption capacities towards Congo-Red dye, twice and five times as much as Ca and Na-montmorillonite, respectively [82].

The batch adsorption experimental data were fitted to the Langmuir and Freundlich isotherm models (Table 5). The regression analysis results showed that the Langmuir isotherm was able to describe the adsorption of RR120 onto natural-Fouchana and HDTMA-Fouchana more accurately than the Freundlich model. Langmuir model assumes that the surface is homogenous which indicates that available active sites are homogenously distributed on Fouchana clay surfaces according to the good fit of data by this model. One can notice that the clay surface coverage by dye is still a monolayer although the amount of dye adsorbed onto HDTMA is larger.

3.2.4. *Effect of additives*

The effect of additives was studied at the maximum initial concentration of dye defined from the experiment described previously (§ 3.2.3) i.e. 30 mg/L for the unmodified clay and 80 mg/L for HDTMA-Fouchana, and at the natural pH conditions of the initial solutions (Table 6). From Fig. 6 it appears that a great amount of initial dye may be adsorbed than what was observed in the experiment without additives. This is the case with the additives Cotoblanc (5.51 mg/g), Bactosol (6.05 mg/g), CHT Catalase (6.16 mg/g), and Kollasol (6.47 mg/g). The maximum amount adsorbed was recorded when all additives are mixed with the dye (7.07 mg/g). A lower amount of adsorbed dye was however recorded for the additives Duralkan and Meropan (3.39 and 4.41 mg/g respectively). These results indicate that most of the additives enhanced the adsorption of dye onto the natural clay and that altogether seem to have had a synergistic effect which allowed further adsorption of dye compared to that of the additives taken separately. Moreover, the initial concentration of dye may be set at higher value than 30 mg/L without reaching the limit recorded in the experiment without additives. Contrary to what occurred in the experiment with the

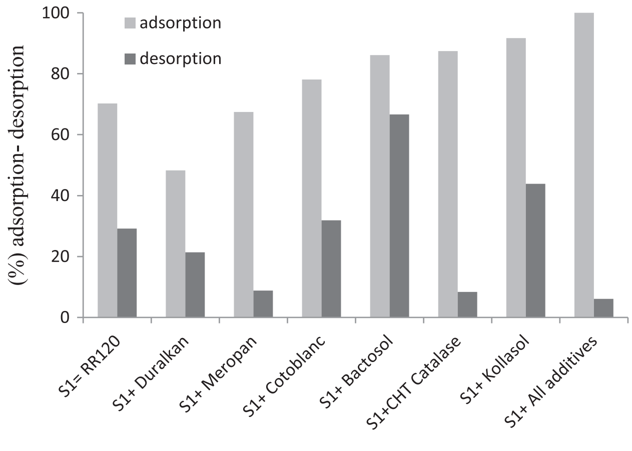

Fig. 6. Effect of additives on the adsorption and desorption of RR120 dye with unmodified clay ($C_0 = 30$ mg/L, *T* = 25˚C, pH of initial solution (Table 6)).

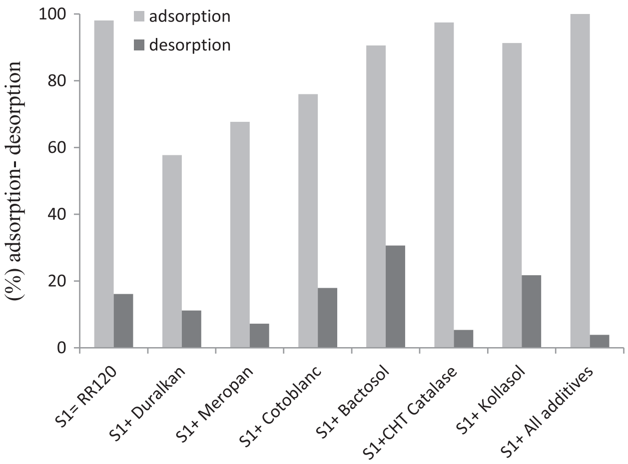

Fig. 7. Effect of additives on the adsorption and desorption of RR120 dye with HDTMA modified clay ($C_i = 80$ mg/L, $T = 25$°C, pH of initial solution (Table 6)).

unmodified clay, additives did not enhance adsorption of dye onto HDTMA-Fouchana (Fig. 7). For most of additives, there was a decrease in the amount of dye adsorbed compared to the experience without additives. This indicates that most of additives hinder the adsorption of dye onto HDTMA-Fouchana. These molecules either compete with the dye ions for adsorption sites on HDTMA-clay and are preferentially adsorbed, or coat the dye ions and prevent adsorption.

The desorption rate was calculated relative to the maximum adsorption rate observed when all additives were added. The desorption rate with both clays varied in function of the additive (Figs. 6 and 7). In case of unmodified Fouchana clay, the desorption rate it was very high in case of added Bactosol and Kollasol which enhanced the adsorption of dye. It was however low in case of CHT Catalase and when all additives were present (Fig. 6). That means that some additives which showed an efficiency for adsorption, have a weak effect on dye sequestration, but again all additives together seem to have a synergic effect in efficient dye sequestration on the clay.

In the case of HDTMA-Fouchana clay, there was no significant improvement in the amount of adsorbed dye when all additives were present. However, the desorption rate was lower which means that additives had at least the role of sequestration of dye adsorbed onto clay (Fig. 7).

3.2.5. Effect of non-clay minerals in Fouchana bulk sample

Previous effluent adsorption experiments were performed using the bulk Fouchana clay which showed the efficiency of color removal although minor minerals, such as quartz, calcite, and gypsum were present [55]. Here we performed batch experiments using the bulk fraction of Fouchana which contains non-clay minerals, RR120 dye at the initial concentration of 80 mg/L as for the experiments with HDTMA-Fouchana, and the additives. The results are compared in Fig. 8. As for the previous experiments the amount of dye adsorbed by HDTMA-Fouchana without additives was much higher than for the unmodified Fouchana. However it appeared that the Fouchana bulk sample adsorbed more dye (12.24 mg/g) than previously recorded (around 8 mg/g). When all additives were

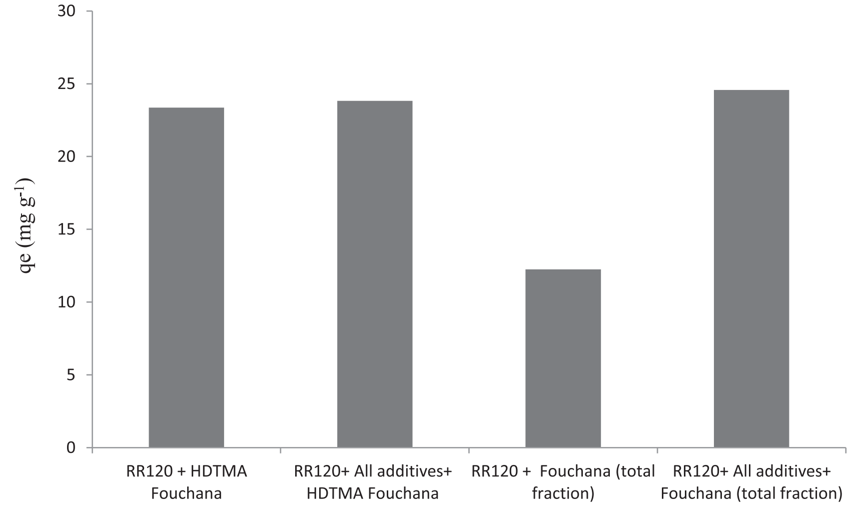

Fig. 8. Effect of additives on the adsorption of RR120 dye onto Fouchana-modified clay and total fraction of natural clay ($C_i = 80$ mg/L, $T = 25$°C, pH of initial solution (Table 6)).

added the amount adsorbed was much higher and equal to that recorded for HDTMA-Fouchana (22.75 mg/L). These results show again that additives strongly enhance adsorption on unmodified clay. But it also points out that adsorption is possible at an initial concentration of dye higher than what was determined in the experience without additives. Furthermore, non-clay minerals do not hinder adsorption but it seems rather the opposite: they probably furnish additional adsorption sites to the anionic dye.

3.3. FTIR analysis of RR120/Fouchana/additives

FTIR analyses were performed to highlight interactions in the system clay-RR120 dye-additives (Fig. 9(a)–(d)). Two additives were selected for which interaction could be identified, and also in order to represent (1) one of the best cases in adsorption improvement (Bactosol), and (2) one of the worst cases of adsorption (Duralkan). Moreover, the pattern for the interaction of clay and RR120 with all six additives together is also given in Fig. 9.

The spectrum of Fouchana clay shows a band at 420 cm^{-1} due to the deformation of [Si–O–Fe] (Fig. 7(a)). The adsorption bands at 470 and 535 cm^{-1} can be assigned, respectively, to [Si–O–Mg] and [Si–O–Al] and indicate that there has been substitution of Al^{3+} by Mg^{2+} in the octahedral sites [83]. The valence and deformation bands at 3,641 and 914 cm^{-1} correspond to the vibrations Al–Al–OH, and show that the clay is dioctahedral [84] and more precisely that it is a dioctahedral smectite [85]. The deformation bands at 695 and 3,715 cm^{-1} show the presence of

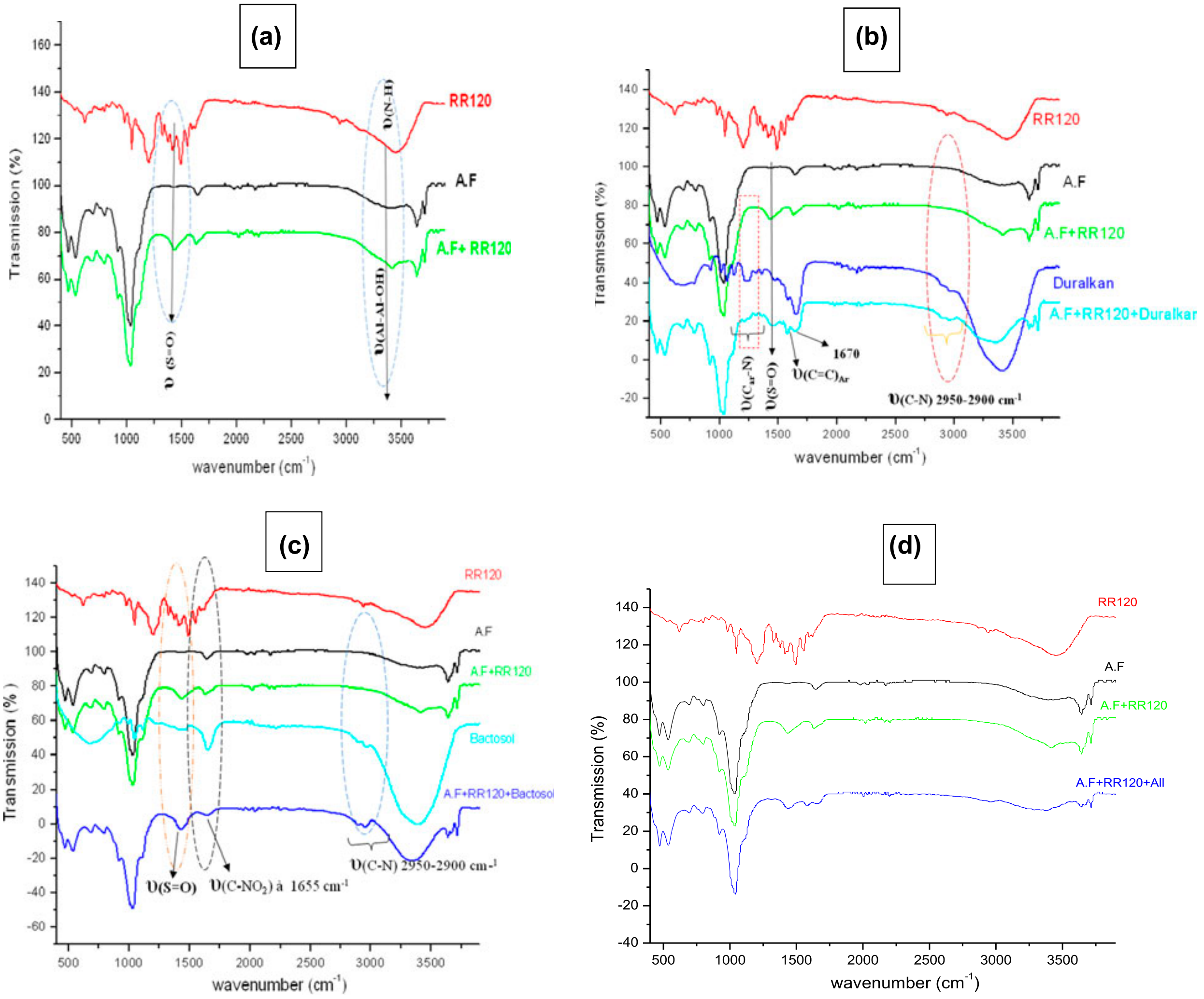

Fig. 9. IR spectra of (a) Fouchana clay (AF) before adsorption, RR120 dye and RR120 adsorbed onto Fouchana clay without additives, (b) with the additive Duralkan, (c) with the additive Bactosol, and (d) with the mixture of all additives.

kaolinite [86]. The bands at 3,362 and 1,644 cm^{-1} are attributed to the vibration of the O–H group of the hydration water of the clay network. These vibrational bands overlap with those of the hydration water of the interlayer cations. Quartz is present and characterized by the band at 801 cm^{-1} [83]. The strong band at 1,036 cm^{-1} represents the Si–O group in plane and out of plane **[87]**.

Interaction between Fouchana clay and adsorbed RR120 dye (Fig. 9(a)) is characterized by a slight intensity increase of the Al–Al–OH group characteristic band from the clay network; this is probably due to the interaction by hydrogen bonds with the N–H group of RR120. Moreover the appearance of the absorption band around 1,450 cm^{-1} specific of S=O group confirms the sequestration of RR120 by the clay matrix.

After adsorption of RR120 on clay in the presence of additives, IR spectra show noticeable interactions with Duralkan and Bactosol. For Duralkan (Fig. 9(b)) the IR spectrum shows several changes compared to the spectra of clay only and RR120 adsorbed on clay; they are listed as follows:

(1) There is an extension of the characteristic band of the clay OH group; this vibration band moves from 1,625 towards 1,670 through interaction with the (C=N) group of the Duralkan molecule.
(2) Two absorption bands appear at 2,950 and 2,900 cm^{-1} which are specific of the C–N group and indicate the sequestration of the Duralkan molecule by the clay matrix.
(3) The band around 1,450 cm^{-1}-specific of the dye (S=O) group suggests that it also interferes with the clay even in the presence of the Duralkan additive.
(4) There is a widening of the vibration band towards 3,400 cm^{-1} of the clay Al–Al–OH group by interaction with the (N–H) group of Duralkan molecule.
(5) The absorption bands appearing in the wave range from 1,470 to 1,100 cm^{-1} confirm the interaction of the (C_{ar}–N) group of Duralkan with the clay lattice.

IR spectrum of RR120 adsorbed on clay with Bactosol additive (Fig. 9(c)) shows a broad characteristic band of the clay OH group which is probably due to the interaction with the C–NO_2 group of the Bactosol molecule (hydrogen bond). Also, the appearance of two absorption bands at 2,950 and 2,900 cm^{-1} specific of the group C–N confirms the sequestration of the Bactosol molecule by the clay matrix. Moreover, the band around 1,450 cm^{-1} specific of the group S=O of the RR120 dye indicates that it also interferes with the clay even in the presence of the additive Bactosol.

The IR spectrum of the clay after adsorption of the dye with the mixture of all additives shows absorption bands specific to some functional Duralkan groups indicating that these molecules interfere with the clay network (Fig. 9(d)) even when mixed with the other additives.

4. Conclusion

The adsorption of RR120 onto natural and organophilic clays investigated in aqueous solution showed that the organophilic clay fixed more RR120 than the natural clay. The adsorption isotherms of both clays were best fitted by Langmuir adsorption isotherm that assumes that dye molecules formed monolayers over the homogenous surfaces of adsorbent. The large amounts of dye molecules adsorbed on HDTMA-Fouchana still form a monolayer onto the clay surfaces. The pseudo-second-order kinetic model fits the best to the experimental data.

Different adsorption trends are evidenced when textile dyeing additives are present. The adsorption of RR120 anionic dye is, on the overall, strongly enhanced in case of Fouchana unmodified clay contrary to the modified clay for which a reduction was mostly recorded. Furthermore, adsorption may be possible at initial concentration of dye higher than what was initially set in our experiments. Moreover, the bulk Fouchana material presents properties for adsorption of anionic dye when additives are added, comparable that of the clay modified with HDTMA. Thus, separation of the <2 μm fraction of clay is not necessary to achieve an efficient adsorption and nonclay minerals do not hinder RR120 dye adsorption. On the contrary, there is an improvement of dye adsorption in presence of all additives.

These results show that textile dyeing effluents containing dyes and additives may be treated by bulk natural clay without separation of the <2 μm fraction or modifying the surface charge by surfactants.

Acknowledgments

This work was done in the frame of the PHC UTIQUE French-Tunisian project (12G21002) with the support from the French Ministries of Foreign Affairs (MAE) and Education and Research (MESR), and the Tunisian Minister of Higher Education and Scientific Research. The authors thank the CITET for their analytical contribution, and F. Huber, A. Aubert, and J.L. Cézard from the mineralogy laboratory of LHYGES.

References

[1] F.A. Batzias, D.K. Sidiras, Dye adsorption by prehydrolysed beech sawdust in batch and fixed-bed systems, Bioresour. Technol. 98 (2007) 1208–1217.

[2] Y. Li, J.-Q. Shi, R.-J. Qu, M.-B. Feng, F. Liu, M. Wang, Z.-Y. Wang, Toxicity assessment on three direct dyes (D-BLL, D-GLN, D-3RNL) using oxidative stress bioassay and quantum parameter calculation, Ecotoxicol. Environ. Saf. 86 (2012) 132–140.

[3] I. Bazin, A. Ibn Hadj Hassine, Y. Haj Hamouda, W. Mnif, A. Bartegi, M. Lopez-Ferber, M. De Waard, C. Gonzalez, Estrogenic and anti-estrogenic activity of 23 commercial textile dyes, Ecotoxicol. Environ. Saf. 85 (2012) 131–136.

[4] B. de Campos Ventura-Camargo, P. Pasquali Parise Maltempi, M. Aparecida Marin-Morales, The use of the cytogenetic to identify mechanisms of action of an azo dye in Allium Cepa Meristematic Cells, J. Environ. Anal. Toxicol. 1(3) (2011) 1–3.

[5] G. Al, U. Özdemir, Ö. Aksoy, Cytotoxic effects of Reactive Blue 33 on *Allium cepa* determined using Taguchi's L8 orthogonal array, Ecotoxicol. Environ. Saf. 98 (2013) 36–40.

[6] R.D. Combes, R.B. Haveland-Smith, A review of the genotoxicity of food, drug and cosmetic colours and other azo, triphenylmethane and xanthene dyes. Mutat. Res. Rev. Genet. Toxicol. 98 (1982) 101–243.

[7] J.R. Easton, The dye-makers view, in: P. Cooper (Ed.), Colour in Dyehouse Effluent, Society of Dyers and Colourists, Bradford, 1995, pp. 9–21.

[8] E.A. Sweeney, J.K. Chipman, S.J. Forsythe, Evidence for direct-acting oxidative genotoxicity by reduction products of azo dyes, Environ. Health Perspect. 102 (Suppl. 6) (1994) 119–122.

[9] F.-M. Chequer, T. Lizier, R. de Felício, M. Zanoni, H.-M. Debonsi, N. Lopes, R. Marcos, D. de Oliveira, Analyses of the genotoxic and mutagenic potential of the products formed after the biotransformation of the azo dye Disperse Red 1, Toxicol. Vitro 25 (2011) 2054–2063.

[10] E. Demirbas, M. Kobya, M.T. Sulak, Adsorption kinetics of a basic dye from aqueous solutions onto apricot stone activated carbon, Bioresour. Technol. 99 (2008) 5368–5373.

[11] X.-F. Sun, S.-G. Wang, X.-W. Liu, W.-X. Gong, N. Bao, B.-Y. Gao, H.-Y. Zhang, Biosorption of malachite green from aqueous solutions onto aerobic granules: Kinetic and equilibrium studies, Bioresour. Technol. 99 (2008) 3475–3483.

[12] N. Emanuel, G. Kumar, Photo detoxification of solubilized vat dye effluent using different pH ranges, Environ. Chem. Lett. 7 (2009) 375–379.

[13] F. Edelin, L'épuration physico-chimique des eaux [The Physicochemical Epuration of Water], Edition Cebedoc, Liège, 1998.

[14] L. El Kbir, M. El Krati, A. Abouzaid, Epuration physico-chimique des rejets liquides de l'industrie textile (Zone industrielle d'El Jadida — Maroc), L'eau, l'industrie, les nuisances 214 (1998) 54–60.

[15] A. Mittal, R. Jain, J. Mittal, S. Varshney, S. Sikarwar, Removal of Yellow ME 7 GL from industrial effluent using electrochemical and adsorption techniques, Int. J. Environ. Pollut. 43 (2010) 308–323.

[16] V.K. Gupta, R. Jain, A. Mittal, T.A. Saleh, A. Nayak, S. Agarwal, S. Sikarwar, Photo-catalytic degradation of toxic dye amaranth on TiO_2/UV in aqueous suspensions, Mater. Sci. Eng. C 32 (2012) 12–17.

[17] S. Pannuzo, A. Serre, Traiter l'eau et les effluents industriels par les techniques membranaires et d'autres techniques couplées, L'eau, l'industrie, les nuisances 235 (2000) 123–128.

[18] A. Bes-Piá, J.A. Mendoza-Roca, M.I. Alcaina-Miranda, A. Iborra-Clar, M.I. Iborra-Clar, Combination of physico-chemical treatment and nanofiltration to reuse wastewater of a printing, dyeing and finishing textile industry, Desalination 157 (2003) 73–80.

[19] R.S. Juang, F.C. Wu, R.L. Tseng, The ability of activated clay for the adsorption of dyes from aqueous solutions, Environ. Technol. 18 (1997) 525–531.

[20] K.S. Low, C.K. Lee, Quaternized rice husk as sorbent for reactive dyes, Bioresour. Technol. 61(2) (1997) 121–125.

[21] M. Ahmaruzzaman, V.K. Gupta, Rice husk and its ash as low-cost adsorbents in water and wastewater treatment, Ind. Eng. Chem. Res. 50(24) (2011) 13589–13613.

[22] Y. Chen, Y. Zhao, J. Chen, K. Zhuo, J. Wang, C. Jiao, M. Feng, Aggregation behavior of a model ionic liquid surfactant in monosaccharide+water solutions, J. Colloid Interface Sci. 364(2) (2011) 388–394.

[23] A.G.L. Abdullah, M.A.M. Salleh, M.K.S. Mazlina, M.J.M.M. Noor, M.R. Osman, R. Wagiran, S. Sobri, Azo dye removal by adsorption using waste biomass sugarcane biogases, Int. J. Eng. Technol. 1(2) (2005) 8–13.

[24] M.C. Ncibi, B. Mahjoub, M. Seffen, Adsorptive removal of textile reactive dye using *Posidonia oceanica* (L.) fibrous biomass, Int. J. Environ. Sci. Technol. 4(4) (2007) 433–440.

[25] K.G. Bhattacharyya, A. Sarma, Adsorption characteristics of the dye, Brilliant Green, on Neem leaf powder, Dyes Pigm. 57 (2003) 211–222.

[26] A.P.S. Immich, A.A. Ulson de Souza, S.M. de A.G. Ulson de Souza, Removal of Remazola Blue RR dye from aqueous solution with neem leaf and evaluation of their acute toxicity with daphnia magna, J. Hazard. Mater. 164 (2009) 1580–1585.

[27] T. Robinson, B. Chandran, P. Nigam, Removal of dyes from a synthetic textile dye effluent by biosorption on apple pomace and wheat straw, Water Res. 36 (2002) 2824–2830.

[28] P. Pandit, S. Basu, Removal of ionic dyes from water by solvent extraction using reverse micelles, Environ. Sci. Technol. 38 (2004) 2435–2442.

[29] V.K. Gupta, R. Jain, S. Varshney, Electrochemical removal of the hazardous dye Reactofix Red 3 BFN from industrial effluents, J. Colloid Interface Sci. 312 (2) (2007) 292–296.

[30] V.K. Gupta, I. Ali, V.K. Saini, Defluoridation of wastewaters using waste carbon slurry, Water Res. 41(15) (2007) 3307–3316.

[31] A. Mittal, V.K. Gupta, A. Malviya, J. Mittal, Process development for the batch and bulk removal and recovery of a hazardous, water-soluble azo dye (Metanil Yellow) by adsorption over waste materials (Bottom Ash and De-Oiled Soya), J. Hazard. Mater. 151(2–3) (2008) 821–832.

[32] A.K. Jain, V.K. Gupta, A. Bhatnagar, A comparative study of adsorbents prepared from industrial wastes for removal of dyes, Sep. Sci. Technol. 38(2) (2003) 463–481.

[33] A. Mittal, Removal of the dye, Amaranth from Waste water using hen feathers as potential adsorbent, Electron. J. Environ. Agric. Food Chem. 5(2) (2006) 1296–1305.

[34] A. Mittal, J. Mittal, A. Malviya, V.K. Gupta, Removal and recovery of Chrysoidine Y from aqueous solutions by waste materials, J. Colloid Interface Sci. 344 (2) (2010) 497–507.

[35] V.K. Gupta, S.K. Srivastava, D. Mohan, S. Sharma, Design parameters for fixed bed reactors of activated carbon developed from fertilizer waste for the removal of some heavy metal ions, Waste Manage. 17 (8) (1998) 517–522.

[36] A. Mittal, D. Kaur, A. Malviya, J. Mittal, V.K. Gupta, Adsorption studies on the removal of coloring agent phenol red from wastewater using waste materials as adsorbents, J. Colloid Interface Sci. 337(2) (2009) 345–354.

[37] A. Mittal, J. Mittal, A. Malviya, D. Kaur, V.K. Gupta, Decoloration treatment of a hazardous Triarylmethane dye, Light Green SF (Yellowish) by waste material adsorbents, J. Colloid Interface Sci. 342(2) (2010) 518–527.

[38] A.K. Jain, V.K. Gupta, A. Bhatnagar, S. Jain, S. Suhas, Comparative assessment of adsorbents prepared from industrial wastes for the removal of cationic dye, J. Indian Chem. Soc. 80(4) (2003) 267–270.

[39] A. Mittal, V.K. Gupta, Adsorptive removal and recovery of the azo dye Eriochrome Black T, Toxicol. Environ. Chem. 92(10) (2010) 1813–1823.

[40] V.K. Gupta, R. Jain, A. Mittal, T.A. Saleh, A. Nayak, S. Agarwal, S. Sikarwar, Photo-catalytic degradation of toxic dye Amaranth on TiO_2/UV in aqueous suspensions, Mater. Sci. Eng. C 32 (2012) 12–17.

[41] A. Mittal, J. Mittal, A. Malviya, V.K. Gupta, Adsorptive removal of hazardous anionic dye "Congo red" from wastewater using waste materials and recovery by desorption, J. Colloid Interface Sci. 340(1) (2009) 16–26.

[42] A. Mittal, J. Mittal, A. Malviya, D. Kaur, V.K. Gupta, Adsorption of hazardous dye crystal violet from wastewater by waste materials, J. Colloid Interface Sci. 343(2) (2010) 463–473.

[43] A. Mittal, J. Mittal, L. Kurup, Utilization of hen feathers for the adsorption of a hazardous dye Indigo Carmine from its simulated effluent, J. Environ. Prot. Sci. 1 (2007) 92–100.

[44] A. Mittal, D. Jhare, J. Mittal, V.K. Gupta, Batch and bulk removal of hazardous colouring agent Rose Bengal by adsorption over bottom ash, RSC Adv. 2(22) (2012) 8381–8389.

[45] A. Mittal, R. Jain, J. Mittal, S. Varshney, S. Sikarwar, Removal of Yellow ME 7 GL from industrial effluent using electrochemical and adsorption techniques, Int. J. Environ. Pollut. 43(4) (2010) 308–323.

[46] A. Mittal, R. Jain, J. Mittal, M. Shrivastava, Adsorptive removal of hazardous dye Quinoline Yellow from waste water using coconut-husk as potential adsorbent, Fresenius Environ. Bull. 19(6) (2010) 1–9.

[47] V.K. Gupta, A. Rastogi, A. Nayak, Biosorption of nickel onto treated alga (*Oedogonium hatei*): Application of isotherm and kinetic models, J. Colloid Interface Sci. 342(2) (2010) 533–539.

[48] V.K. Gupta, A. Mittal, A. Malviya, J. Mittal, Adsorption of Carmoisine A from wastewater using waste materials—Bottom ash and deoiled soya, J. Colloid Interface Sci. 335(1) (2009) 24–33.

[49] M. Roulia, A.A. Vassiliadis, Interactions between C.I. Basic Blue 41 and aluminosilicate sorbents, J. Colloid Interface Sci. 291 (2005) 37–44.

[50] Z. Li, R.S. Bowman, Sorption of chromate and PCE by surfactant-modified clay minerals, Environ. Eng. Sci. 15 (1998) 237–245.

[51] B.S. Krishna, D.S.R. Murty, B.S. Jai Prakash, Thermodynamics of chromium(VI) anionic species sorption onto surfactant-modified montmorillonite clay, J. Colloid Interface Sci. 229 (2000) 230–236.

[52] Z. Li, R.S. Bowman, Retention of inorganic oxyanions by organo-kaolinite, Water Res. 35(16) (2001) 3771–3776.

[53] J. Behnsen, B. Riebe, Anion selectivity of organobentonites, Appl. Geochem. 23 (2008) 2746–2752.

[54] M.M. Mortland, S. Shaobai, S.A. Boyd, Clay-organic complexes as adsorbents for phenol and chlorophenols1, Clays Clay Miner. 34 (1986) 581–585.

[55] E. Errais, Réactivité de surface d'argiles naturelles [Surface Reactivity of Natural Clays], PhD Thesis, Strasbourg University, France, Etude de l'adsorption de colorants anioniques, 2011.

[56] E. Errais, J. Duplay, F. Darragi, Textile dye removal by natural clay—case study of Fouchana Tunisian clay, Environ. Technol. 31 (2010) 373–380.

[57] E. Errais, J. Duplay, F. Darragi, I. M'Rabet, A. Aubert, F. Huber, G. Morvan, Efficient anionic dye adsorption on natural untreated clay: Kinetic study and thermodynamic parameters, Desalination 275 (2011) 74–81.

[58] E. Errais, J. Duplay, M. Elhabiri, M. Khodja, R. Ocampo, R. Baltenweck-Guyot, F. Darragi, Anionic RR120 dye adsorption onto raw clay: Surface properties and adsorption mechanism, Colloids Surf. A 403 (2012) 69–78.

[59] S. Brunauer, P.H. Emmett, E. Teller, J. Am. Chem. Soc. 60 (1938) 309–319.

[60] AFNOR, NF X 31-130 soil quality, Chemical methods, Determination of Cation Exchange Capacity (CEC) and Cation Extraction, AFNOR, Paris, 1999.

[61] H. Van Olphen, An Introduction to Clay Colloid Chemistry, Wiley Interscience Publishers, New York, NY, 1963.

[62] P. Baskaralingam, M. Pulikesi, D. Elango, V. Ramamurthi, S. Sivanesan, Adsorption of acid dye onto organobentonite, J. Hazard. Mater. 128 (2006) 138–144.

[63] M. Kumar, S.K. Chinta, D. Kumar, Adsorption and thermodynamic study of pigment dyeing on cationised cotton, Int. J. Fiber Text. Res. 2013. Available from: <www.urpjournals.com>.

[64] M.M. Kamel, M.M. El Zawahry, N.S.E. Ahmed, F. Abdelghaffar, Ultrasonic dyeing of cationized cotton fabric with natural dye. Part 2: Cationization of cotton using Quat 188, Ind. Crops Prod. 34 (2011) 1410–1417.

[65] S. Lagergren, About the theory of so-called adsorption of soluble substances, K. Sv. Vet.-Akad. Handl. Band. 24 (1898) 1–39.

[66] K.G. Bhattacharyya, A. Sharma, Azadirachta indica leaf powder as an effective biosorbent for dyes: A case study with aqueous Congo Red solutions, J. Environ. Manage. 71 (2004) 217–229.

[67] R. Gündoğan, B. Acemioğlu, M.H. Alma, Copper (II) adsorption from aqueous solution by herbaceous peat, J. Colloid Interface Sci. 269 (2004) 303–309.

[68] D. Yue, Y. Jing, J. Ma, C. Xia, X.Y.Y. Yin, Removal of neutral red from aqueous solution by using modified hectorite, Desalination 267 (2011) 9–15.

[69] S.J. Elovich, The nature of the chemisorption of carbon monoxide on manganese dioxide, in: J.H. Schulman (Ed.), Proceedings of the Second International Congress of Surface Activity, Butterworths Scientific publications, London, 1957, pp. 252–259.

[70] I. Langmuir, The adsorption of gases on plane surfaces of glass, mica and platinum, J. Am. Chem. Soc. 40 (1918) 1361–1403.

[71] B.H. Hameed, J.M. Salman, A.L. Ahmad, Adsorption isotherm and kinetic modeling of 2,4-d pesticide on activated carbon derived from date stones, J. Hazard. Mater. 163 (2009) 121–126.

[72] Y. Ho, J. Porter, G. McKay, Equilibrium isotherm studies for the sorption of divalent metal ions onto peat: Copper, nickel and lead single component systems, Water Air Soil Pollut. 141 (2002) 1–33.

[73] R.E. Treybal, Mass Transfer Operations, 3rd ed., McGraw Hill, New York, NY, 1980.

[74] G.M. Brindley, G. Brown, Crystal Structures of Clay Minerals and their X-ray Identification, Mineralogical Society Monograph No. 5, Mineralogical Society, London, 1980.

[75] P.G. Slade, W.P. Gates, The swelling of HDTMA smectites as influenced by their preparation and layer charges, Appl. Clay Sci. 25 (2004) 93–101.

[76] O. Bouras, Propriétés adsorbantes d'argiles pontées organophiles: synthèse et caractérisation [Adsorptive Properties of Organophilic Pillared Clays: Synthesis and Characterization], PhD Thesis, University of Limoges, France, 2003.

[77] G.A. Ikhtiyarova, A.S. Özcan, Ö. Gök, A. Özcan, Characterization of natural and organobentonite by XRD, SEM, FT-IR and thermal analysis techniques and its adsorption behaviour in aqueous solutions, Clay Miner. 47 (2012) 31–44.

[78] L.-C. Juang, C.-C. Wang, C.-K. Lee, T.-C. Hsu, Dyes adsorption onto organoclay and MCM-41, Environ. Eng. Manage. 17 (2007) 29–38.

[79] G. Sposito, Surface reaction in natural colloidal system, CHIMIA 43 (1989) 169–176.

[80] S. Elemen, E.P.A. Kumbasar, S. Yapar, Modeling the adsorption of textile dye on organoclay using an artificial neural network, Dyes Pigm. 95 (2012) 102–111.

[81] N.P. Jović-Jovičić, A.D. Milutinović-Nikolić, M.J. Žunić, Z.D. Mojović, P.T. Banković, I.A. Gržetić, D.M. Jovanović, Synergic adsorption of Pb^{2+} and reactive dye—RB5 on two series of organomodified bentonites, J. Contam. Hydrol. 150 (2013) 1–11.

[82] X. Yu, C. Wei, L. Ke, Y. Hu, X. Xie, H. Wu, Development of organovermiculite-based adsorbent for removing anionic dye from aqueous solution, J. Hazard. Mater. 180 (2010) 499–507.

[83] H.W. Van der Marel, H. Beutlspacher, Atlas of infrared spectroscopy of clay minerals and their admixtures, Elseiver Scientific Publishing Company, Amsterdam, 1976.

[84] S. Caillère, S. Hénin, M. Rautureau, Minéralogie des argiles [Clay Mineralogy], Tomes 1 et 2, Masson, Paris, 1982.

[85] J.B. Dixon, S.B. Weed, Minerals in Soil environment, Published by Soil Science Society of America, Madeson, WI, 1977.

[86] W.M. Tuddenham, R.J.P. Lyon, Infrared techniques in the identification and measurement of minerals, Anal. Chem. 32 (1960) 1630–1634.

[87] V.C. Farmer, J.D. Russell, The infra-red spectra of layer silicates, Spectrochim. Acta 20 (1964) 1149–1173.